# Efficient Removal Of Congo Red Using Nickel Iron Modified Layered Double Hydroxide As Adsorbent

**Neza Rahayu Palapa, Tarmizi Taher, Arini Fousty Badri, Risfidian Mohadi, Aldes Lesbani**

**Abstract:** The removal of anionic congo red dye by adsorption was studied using Ni/Fe and Ni/Fe-POM layered double hydroxides (LDHs). Material Ni/Fe LDH was prepared using the coprecipitation method at pH 10. Material Ni/Fe LDH was intercalated using polyoxometalate (POM) silicotungstic to form Ni/Fe-POM LDHs. The LDHs were characterized using XRD, FTIR, and BET analyses. The adsorption parameters such as kinetic and thermodynamic adsorption were investigated. Adsorption of congo red on both LDHs follows the pseudo-second-order kinetic model. The thermodynamic adsorption of congo red on Ni/Fe and Ni/Fe-POM LDHs shows spontaneous, endothermic adsorption process and adsorption was classify as physical adsorption.

**Index Terms**: Layered Double Hydroxides, Ni/Fe, Ni/Fe-POM, Congo Red, Adsorption

## 1. INTRODUCTION

ENVIRONMENTAL pollution has been an intriguing topic until this decade. One of the toxic pollutants in the environment is dyes. Dyes contamination in the environment is resulting from industrial activities such as textiles, paintings, plastics, papers, wools, leathers, and so on [1]. The existence of dyes in the natural water causes a carcinogenic hazard on human and flora fauna of the environment. The removal of dyes from wastewater is still conducted until this time by various methods such as coagulation [2], filtration [3], and adsorption [4]. Among these methods, adsorption has several advantages due to simple operation, low cost, and efficient to remove dyes from solution [5-6]. The successful process of adsorption depends on the properties of adsorbent. Various kinds of adsorbents have been applied to remove dyes from an aqueous solution such as chitosan [7], cellulose [8], zeolite [9], kaolinite [10], bentonite [11], montmorillonite [12], and layered double hydroxide materials [13-14]. Layered double hydroxide (LDH) is inorganic materials with well-ordered layer structure with the general formula $[M^{2+}_{1-x}M^{3+}_{x}(OH)_2]^{x+}(A^{n-})_{x/n}]\cdot nH_2O$, where $M^{2+}$ is divalent metal ions, $M^{3+}$ is trivalent metal ions and An- is interlayer anions with valence n [15]. The structure of LDH with positive charging of the layer is resulting from the partial substitution of the divalent metal ion by trivalent metals ion in the layer. Anion in the interlayer space is balancing the charge of LDH [16]. Various divalent and trivalent metal ions have been tested for formation of LDH such as $M^{2+}$ =$Mg^{2+}$, $Ca^{2+}$, $Zn^{2+}$, $Ni^{2+}$, $Cu^{2+}$, $Co^{2+}$ and $M^{3+}$ = $Al^{3+}$, $Fe^{3+}$, $Cr^{3+}$, $V^{3+}$. Anion in the interlayer space can be carbonate, nitrate, chloride, or sulfate, depending on the synthetic precursor of materials [17]. One of the interesting LDH is exchangeable anion in the interlayer space to form unique LDH properties for wide range applications [18]. LDH of Mg-Fe-$CO_3$ has been prepared as an efficient adsorbent of anionic congo red from aqueous solution at low pH [19]. Congo red is anionic dye with azo structure, as shown in Figure 1. Congo red removal from aqueous solution was also removed by Mg-Al LDH. Mg-Al LDH was synthesized at pH 9 and adsorption of congo red was occurred by electrostatic attraction between adsorbent-adsorbate [20]. LDH of Zn-Al was also used as an adsorbent of congo red removal from aqueous solution. Zn-Al LDH can be synthesized using hydrothermal and microwave-assisted hydrothermal methods [21]. LDH was assembly with multi-walled carbon nanotubes from MWCNTs/LDH as adsorbent of congo red. The results showed that MWCNTs/LDH has an excellent adsorption capacity of congo red up to 595.8 mg $g^{-1}$ [22]. On the other hand, adsorption of congo red on Mg-Al-$CO_3$ LDH was an ultrasound-assisted adsorption process with the time-efficient of adsorption [23]. Thus research of congo red removal from aqueous solution using various LDH is still carried out until this time.

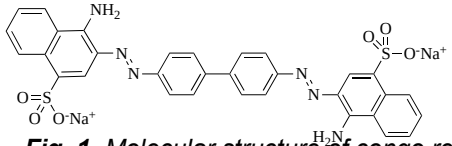

***Fig. 1**. Molecular structure of congo red*

In this research, adsorption of congo red using Ni/Fe and Ni/Fe-POM LDHs were investigated using kinetic and thermodynamic adsorption parameters. Material Ni/Fe LDHs was synthesized using the coprecipitation method, and Ni/Fe-modification was obtained using the intercalation of Ni/Fe with polyoxometalate (POM) silicotungstic. The characterization of LDHs was performed using XRD, FTIR, and BET analyses.

## 2 EXPERIMENTAL SECTION

### 2.1 Chemical and Instrumentations

Chemical reagents were supplied from Merck and Sigma-Aldrich. All chemicals were used directly after purchased. Water was obtained from Purite® water purification system with the ion-exchange method. X-ray powder analysis was conducted using XRD Rigaku Miniflex-600. The sample was


- *Neza Rahayu Palapa and Arini Fousty Badri are doctoral students in Department of Mathematic & Natural Science, Universitas Sriwijaya, Indonesia. E-mail:, nezarahayu@gmail.com , arinifoustybadri@gmail.com*
- *Tarmizi Taher is Postdoctoral Researcher in Institute of Regional Innovation, Hirosaki University, Aomori, Japan. E-mail: tarmizitaher@pps.unsri.ac.id*
- *Risfidian Mohadi is Senior Lecture in department of chemistry, Universitas Sriwijaya. E-mail: risfidian.mohadi@unsri.ac.id*
- *Aldes Lesbani as Corresponding Author is Professor in in Department of Mathematic & Natural Science, Universitas Sriwijaya, Email: aldeslesbani@pps.unsri.ac.id*

grounded with a mortar and was scanned at speed scan 0.1 deg.min$^{-1}$. FTIR spectra were analyzed using the FTIR Prestige-21 spectrophotometer at wavenumber 400-4000 cm$^{-1}$. The sample was mixed with KBr and vacuumed to form a KBr pellet. Surface area analysis was measured using a Quantachrome instrument at 77K. Congo red dye was analyzed using spectrophotometer UV-Vis BioBase BK-UV 1800 PC at wavelength 497 nm. POM $[\alpha\text{-}SiW_{12}O_{40}]^{4-}$ was synthesis according to previous reported [24].

### 2.2 Synthesis of Ni/Fe and Ni/Fe-POM LDHs

Ni/Fe LDH was synthesized according to Ayawei (2015) [25] with slight modification using the coprecipitation method. Solution of nickel(II) nitrate 0.3 M was mixed with a solution of iron(III) nitrate 0.1 M (solution A). The solution of sodium hydroxide 2 M was mixed with a solution of sodium carbonate 1 M (solution B). Solution A was slowly added to solution B and the mixtures were stirred slowly. pH solution was adjusted to pH 10 by adding sodium hydroxide solution to form a solid material. The solid material was dried for 24 hours to obtain Ni/Fe LDH. Material Ni/Fe-POM LDH was synthesis using the ion-exchange method. Compound $K_4[\alpha\text{-}SiW_{12}O_{40}]$ was dissolved with water (solution A). Material Ni/Fe LDH was mixed with a solution of sodium hydroxide (solution B). Solution A was mixed with solution B under nitrogen atmospheric conditions at 40 $^{o}$C for 24 hours to obtain solid material of Ni/Fe-POM. The adsorption experiments were studied through adsorption kinetics, adsorption isotherm, and adsorption thermodynamics. The various of initial concentration, adsorption time and temperature batch system were studied. The concentration of MG on solutions after adsorption was measured by a UV–vis spectrophotometer Bio-Base BK-UV 1800 PC at 619 nm.

### 2.3 Analysis of $pH_{PZC}$

Analysis of pH point zero charges (pHpzc) was carried out in wide range pH using hydrochloric acid or sodium hydroxide to a solution of sodium chloride 0.1 M [26]. Hydrochlorid acid or sodium hydroxide solution was added into 0.1 M solution of sodium chloride. pH solution was checked using pH meter. Materials Ni/Fe or Ni/Fe-POM LDHs (0.1 g) were added into these solutions and the mixtures were stirred for 24 hours. The solutions were filtered, and the pH of the filtrate was determined by pH meter. The graph of pHpzc was obtained by comparison initial and final pH solution.

### 2.3 Adsorption Process

Adsorption of congo red was conducted using a batch system. 10 mg of Ni/Fe or Ni/Fe-POM LDHs was added into 25 mL congo red solutions with known concentration. The mixture was stirred at 120 rpm for several minutes. The variation time of adsorption was in the range 10-150 minutes and the filtrate was collected and the concentration of congo red in the aqueous solution was determined by using a UV-Vis spectrophotometer. Kinetic adsorption was obtained by calculation using kinetic model pseudo-first-order and pseudo-second-order using equations 1 and 2 [27-28].
Pseudo first-order kinetic model:

$$\log (q_e\text{-}q_t) = \log q_e - (k_1/2.303)t \qquad (1)$$

where: $q_e$ is adsorption capacity at equlibrium (mg.g$^{-1}$); $q_t$ is adsorption capacity at t (mg.g$^{-1}$); t is adsorption time (minute); and $k_1$ is adsorption kinetic rate at pseudo first-order (minute$^{-1}$).
Pseudo-second-order kinetic model:

$$t/qt = 1/k_2q_e^2 + 1/q_e\, t \qquad (2)$$

where $q_e$ is adsorption capacity at equilibrium (mg.g$^{-1}$); $q_t$ is adsorption capacity at t (mg.g$^{-1}$); t is adsorption time (minute); and $k_2$ is adsorption kinetic rate at pseudo second-order (g.mg$^{-1}$.min$^{-1}$).
Isotherm and thermodynamic adsorption processes were studied by variation of concentration of congo red and temperature adsorption. The concentration of congo red was varied from 20-100 mg.L$^{-1}$ and temperature adsorption in the range 300-328K. Isotherm adsorption was obtained using Freundlich and Langmuir isotherm adsorption model as shown in equations 3 and 4 [29-30].
Langmuir equation:

$$c/m = 1/bK + c/b \qquad (3)$$

where C is a saturated concentration of adsorbate; m is the amount of adsorbate; b is the maximum adsorption capacity (mg.g$^{-1}$), and $K_{ML}$ is the Langmuir constant (L.mg$^{-1}$).
Freundlich equation:

$$\text{Log } q_e = \log K_F + 1/n \log C_e \qquad (4)$$

where $q_e$ is adsorption capacity at equilibrium (mg.g$^{-1}$); $C_e$ is the concentration of adsorbate at equilibrium (mg.L$^{-1}$), and $K_F$ is Freundlich constant.

## 3 RESULTS AND DISCUSSION

### 3.1 Characterization of Adsorbent

The X-ray powder diffraction pattern of Ni/Fe and Ni/Fe-POM LDHs are shown in Figure 2. Ni/Fe LDH has diffraction peak at 11$^{o}$ (003), 23$^{o}$ (006), 34$^{o}$ (110), and 61$^{o}$ (110) [31]. These diffractions suggest the formation of a well-ordered layered structure. The formation of the interlayer is identified at the main diffraction at 11$^{o}$(003), which resulted in interlayer distance 7.67Å. The LDH Ni/Fe-POM after intercalation with POM has diffraction peak at 8$^{o}$, 20-23$^{o}$, 31-36$^{o}$, and 60-61$^{o}$. Diffraction of 003 was shifted to a lower diffraction angle due to the insertion of larger anion of $[\alpha\text{-}SiW_{12}O_{40}]^{4-}$ into the interlayer distance of Ni/Fe LDH. The interlayer distance of Ni/Fe-POM was 10.78 Å, and interlayer distance was increase 3.11Å thus, the intercalation of POM was successfully conducted.

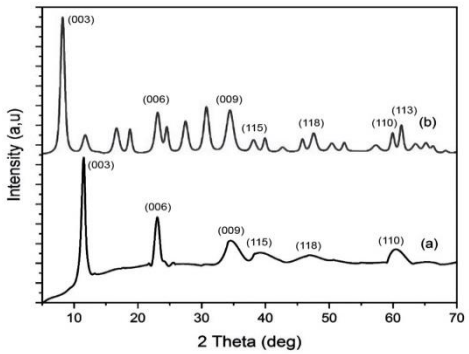


***Fig. 2**. XRD powder pattern of Ni/Fe and Ni/Fe-POM LDHs*

The FTIR spectra of Ni/Fe and Ni/Fe-POM LDHs are shown in Figure 3. The FTIR spectra in Figure 3 are appeared due to water molecules and hydroxyl group, nitrate ion, carbonate ion, divalent and trivalent ions [32-33]. The water molecules in the lattice and interlayer space identified at 3490 $cm^{-1}$. The divalent and trivalent vibration peaks were identified in the range of wavenumber at 400-700 $cm^{-1}$. The peak at 1630 $cm^{-1}$ is also attributed to the water molecules. The weak peak at 1400 $cm^{-1}$ is due to stretching vibration of $CO_3^{2-}$ and peak at 1360 $cm^{-1}$ is assigned as the vibration of nitrate molecules, which comes from synthetic solution. The FTIR spectra of Ni/Fe-POM showed there is main peaks i.e. the peak of POM, the peak of nitrate ion, and the peak of water molecules. The vibration of POM as intercalant was appeared at 900-1150 $cm^{-1}$ due to W=O, W-Oc-W, and W-Oe-W vibrations. The vibration peak of carbonate was disappeared due to the insertion of POM.

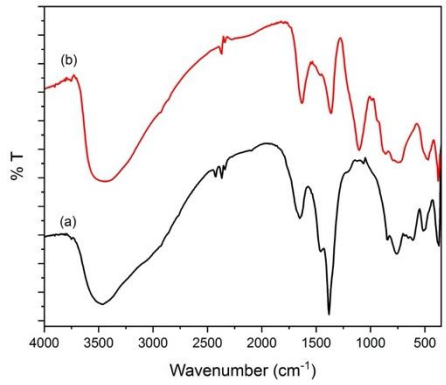


***Fig. 3** FTIR spectra of Ni/Fe and Ni/Fe-POM LDHs*

The nitrogen adsorption-desorption analysis results of Ni/Fe and Ni/Fe-POM LDHs are shown in Figure 4. As shown in Figure 4, the nitrogen adsorption-desorption isotherm was a type IV curve with an H3 hysteresis loop indicating mesoporous materials [34]. The BET analysis was shown in Table 1. There is a significantly increased surface area, pore-volume, and pore diameter of Ni/Fe-POM after the intercalation process indicating the opening of the interlayer distance of layer structure with large ion.

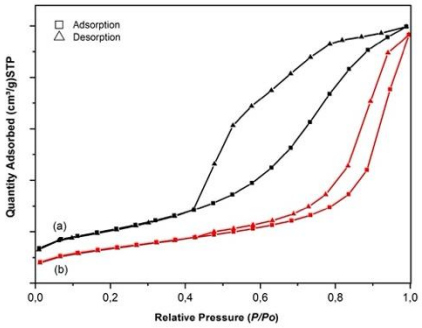


***Fig. 4**. $N_2$ adsorption-desorption on Ni/Fe and Ni/Fe-POM LDHs*

***Table 1.** Textural Properties of Ni/Fe and Ni/Fe-POM LDHs*

| Properties | LDHs | |
|---|---|---|
| | Ni/Fe | Ni/Fe-POM |
| BET Surface Area ($m^2$ $g^{-1}$) | 18.0518 | 55.1425 |
| Pore volume ($cm^3$ $g^{-1}$), BJH | 0.038854 | 0.170438 |
| Pore diameter (nm), BJH | 7.3344 | 13.1352 |

A graph of pHpzc for Ni/Fe and Ni/Fe-POM LDHs are shown in Figure 5. The intersection point for Ni/Fe LDH is at pH 7 and Ni/Fe-POM LDH is at pH 9. The surface charge of LDH below the pHpzc is positively charges and negative charges above pHpzc values. Thus adsorption of congo red is conducted at pH 7 using Ni/Fe LDH and at pH 9 Ni/Fe-POM LDH as adsorbents.

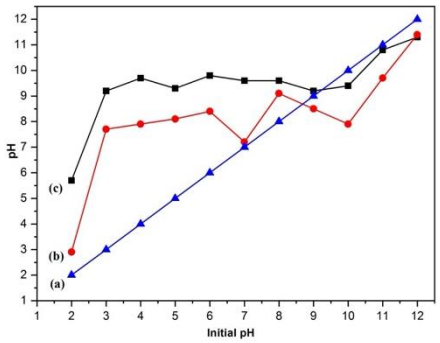


***Fig. 5**. pH pzc graph (a) initial pH, (b) Ni/Fe LDH, (c) Ni/Fe-POM LDH*

Adsorption of congo red on Ni/Fe and Ni/Fe-POM LDHs was firstly investigated using the effect of adsorption time as shown in Figure 6.

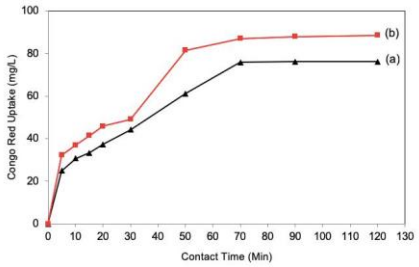


***Fig. 6**. Effect of congo red adsorption time using Ni/Fe (a) and Ni/Fe-POM (b) LDHs*

Figure 6 shows the adsorption of congo red was increased by increasing adsorption time. The adsorption reached equilibrium at 70 minutes for both LDHs. The adsorption amount of Ni/Fe-POM LDH was slightly higher than Ni/Fe LDH as adsorbents. Kinetic adsorption model of pseudo-first-order and pseudo-second-order was applied to obtain the kinetic parameter for adsorption congo red using Ni/Fe and Ni/Fe-POM LDHs. The results of the kinetic parameter are presented in Table 2.

***Table 2.** Adsorption kinetic model of congo red on Ni/Fe and Ni/Fe-POM*

| Kinetic Adsorption Model | Kinetic Parameter | LDH | |
|---|---|---|---|
| | | Ni/Fe | Ni/Fe-POM |
| Pseudo First-Order | $Qe_{Exp}$ (mg $g^{-1}$) | 29.078 | 33.807 |
| | $Qe_{Calc}$ (mg $g^{-1}$) | 78.199 | 28.032 |
| | $R^2$ | 0.784 | 0.812 |
| Pseudo Second-Order | $Qe_{Exp}$ (mg $g^{-1}$) | 29.078 | 33.807 |
| | $Qe_{Calc}$ (mg $g^{-1}$) | 2.099 | 0.002 |
| | $R^2$ | 0.955 | 0.957 |

The kinetic model shows the pseudo-second-order kinetic model is meet for both Ni/Fe and Ni/Fe-POM LDHs as adsorbents. The R values for both adsorbents are close to one.

The effect of temperature on the adsorption of congo red by Ni/Fe and Ni/Fe-POM is shown in Figure 7. In general, the adsorption of congo red was increased by increasing temperature. The isotherm adsorption was analyzed using Freundlich and Langmuir isotherm models as shown in Table 3.

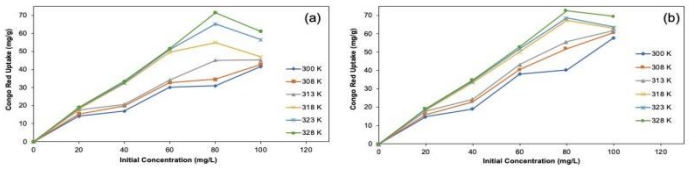


***Fig. 7**. Effect of temperature adsorption and concentration of congo red on Ni/Fe (a) and Ni/Fe-POM (b) LDHs*

Isotherm data in Table 3 showed that adsorption of congo red on Ni/Fe and Ni/Fe-POM LDHs follow the Langmuir isotherm model and the R-value is a close one at a higher temperature. On the other hand, the Freundlich isotherm model fits better than the Langmuir model at lower temperature and adsorption profile as shown in Figure 7 has three steps due to the multilayer adsorption process.

***Table 3.** Isotherm adsorption of congo red on Ni/Fe and Ni/Fe-POM LDHs*

| | Isotherm | Isotherm Paramater | Temperature (K) | | | | | |
|---|---|---|---|---|---|---|---|---|
| | | | 300 K | 308 K | 313 K | 318 K | 323 K | 328 K |
| Ni/Fe LDH | Langmuir | $q_{max}$ (mg $g^{-1}$) | 21.849 | 21.415 | 22.498 | 20.087 | 24.418 | 26.196 |
| | | $k_{ML}$ (L $mg^{-1}$) | 16.146 | 22.533 | 33.123 | 220.653 | 221.255 | 267.002 |
| | | $R^2$ | 0.672 | 0.835 | 0.764 | 0.982 | 0.975 | 0.974 |
| | Freundlich | $k_F$ (mg $g^{-1}$)(L mg)$^{1/n}$ | 2.371 | 3.106 | 4.912 | 7.072 | 7.671 | 8.776 |
| | | n | 2.273 | 2.504 | 3.236 | 3.233 | 2.865 | 2.922 |
| | | $R^2$ | 0.797 | 0.865 | 0.732 | 0.759 | 0.788 | 0.709 |
| Ni/Fe-POM LDH | Langmuir | $q_{max}$ (mg $g^{-1}$) | 36.991 | 45.400 | 33.938 | 28.557 | 27.932 | 30.790 |
| | | $K_{ML}$ (L $mg^{-1}$) | 31.631 | 52.609 | 63.254 | 188.441 | 254.404 | 302.932 |
| | | $R^2$ | 0.291 | 0.395 | 0.527 | 0.969 | 0.976 | 0.966 |
| | Freundlich | $k_F$ (mg $g^{-1}$)(L mg)$^{1/n}$ | 2.040 | 2.447 | 4.677 | 6.906 | 8.285 | 9.173 |
| | | n | 1.711 | 1.657 | 2.321 | 2.404 | 2.703 | 2.636 |
| | | $R^2$ | 0.741 | 0.849 | 0.762 | 0.847 | 0.838 | 0.797 |

The thermodynamic data of the congo red adsorption on Ni/Fe and Ni/Fe-POM LDHs such as a change in free energy (∆G), enthalpy (∆H), and entropy (∆S) is shown in Table 4. The negative value of ∆G indicated adsorption is spontaneous. The positive values of ∆H and ∆S show that the adsorption process was endothermic with increasing in the randomness of the adsorption system. The value of ∆H is less than 100 kJ,$mol^{-1}$ indicated adsorption of congo red on Ni/Fe, and Ni/Fe-POM LDHs is physical adsorption.

***Table 4.** Thermodynamic parameter for adsorption of congo red on Ni/Fe and Ni/Fe-POM LDHs*

| LDH | $\Delta G^o$ (kJ $mol^{-1}$) | | | | | | $\Delta H^o$ (kJ $mol^{-1}$) | $\Delta S^o$ (J $mol^{-1}$ $K^{-1}$) |
|---|---|---|---|---|---|---|---|---|
| | 300 K | 308 K | 313 K | 318 K | 323 K | 328 K | | |
| Ni/Fe | -19.990 | -20.547 | -20.881 | -21.214 | -21.548 | -21.881 | 23.487 | 66.712 |
| Ni/Fe-POM | -10.905 | -11.208 | -11.390 | -11.572 | -11.754 | -11.936 | 12.471 | 36.390 |

## 4 CONCLUSION

Adsorption of congo red on Ni/Fe and Ni/Fe-POM LDHs follow the pseudo-second-order kinetic model. Thermodynamic parameter show adsorption process of congo red was spontaneous, endothermic with increasing randomness of a system. Adsorption of congo red on Ni/Fe and Ni/Fe-POM LDHs was identified as physical adsorption with energy adsorption less than 100 kJ $mol^{-1}$.

## ACKNOWLEDGMENT

Authors thank the Ministry of Research Technology and Higher Education (Kemenristekdikti) Republik Indonesia through "Hibah Penelitian Dasar Unggulan Perguruan Tinggi (PDUPT)" in 2019-2020 fiscal year with contract no. 0060.05/UN9/SB3.LP2M.PT/2019. Authors also thank Research Center of Inorganic Materials and Complexes FMIPA Universitas Sriwijaya for instrumental and analysis support.

## REFERENCES

[1] Y. Zhou, J. Lu, Y. Zhou and Y. Liu. "Recent Advances for Dyes Removal Using Novel Adsorbents: A Review", Environmental Pollution, 252, 352-363, 2019.

[2] H. Li, S. Liu, J. Zhao, and N. Feng. "Removal of Reactive Dyes from Waste water Assisted with Kaolin Clay by Magnesium Hydroxide Coagulation Process". Colloids and Surfaces A: Physicochemical and Engineering Aspects, 494, 222-227, 2016.

[3] P.J. Ong, S.W. Tay, and L. Hong. "Removal of Water-Soluble Dyes by Conjugated Organic Skeletons Through Drain Flow-Diffusion Filtration". Journal of Environmental Chemical Engineering, 6, 4612-4622, 2018.

[4] M.C. Stanciu, and M. Nichifor. "Influence of Dextran Hydrogel Characteristics on Adsorption Capacity for Anionic Dyes". Carbohydrate Polymers, 199, 75-83, 2018.

[5] T.A. Aragaw, and F.T. Angerasa. "Adsorption of Basic

yellow Dye Dataset Using Ethiophian Kaolin as an Adsorbent". Data in Brief, 26, 104504, 2019.

[6] T. Lou, X. Yan, and X. Wang. "Chitosan Coated Polyacrylonitrile Nanofibrous Mat for Dye Adsorption". International Journal of Biological Macromolecules, 135, 919-925. 2019.

[7] M. Sadeghi-Kiakhani, M. Arami. and K. Gharanjig. "Preparation of Chitosan-Ethyl Acrylate as a Biopolymer Adsorbent for Basic Dyes Removal from Colored Solutions". Journal of Environmental Chemical Engineering, 1, 406-415. 2019.

[8] C.H.C. Tan, S. Sabar, and M.H. Hussin. "Development of Immobilized Microcrystalline Cellulose as an Effective Adsorbent for Methylene Blue Dye Removal". South African Journal of Chemical Engineering, 26, 11-24. 2018.

[9] Y. Yu, B.N. Murthy, J.G. Shapter, K.T. Constantopoulos, N.H. Voelcker and A.V. Ellis. "Benzene Carboxylic Acid Derivatized Graphene Oxide Nanosheet on Natural Zeolites as Effective Adsorbents for Cationic Dye Removal". Journal of Hazardous Materials, 260, 330-338. 2013.

[10] N.E.H. Fardjaoui, F.Z.E. Berrichi, and F. Ayari. "Kaolin-Issued Zeolite A as Efficient Adsorbent for Bezanyl Yellow and Nylomine Green Anionic Dyes". Microporous and Mesoporous Materials, 243, 91-101. 2017.

[11] T. Taher. D. Rohendi. R. Mohadi. A. Lesbani. "Thermal and Acid Activation (TAA) of Bentonite as Adsorbent for Removal Methylene Blue: A Kinetics and Thermodynamic Study". Chiang Mai Journal of Science, 45(4), 1770-1781.2018.

[12] C. Puri, and G. Sumana. "Highly Effective Adsorption of Crystal Violet Dye from Contaminated Water Using Graphene Oxide Intercalated Montmorillonite Nanocomposite". Applied Clay Science, 166, 102-112. 2018.

[13] F. Ling, L. Fang, Y. Lu. J. Gao. F. Wu. M. Zhou. and B. Hu. "A Novel CoFe Layered Double Hydroxides Adsorbent: High Adsorption Amount for Methyl Orange Dye and Fast Removal of Cr(VI)". Microporous and Mesoporous Materials, 234, 230-238. 2016.

[14] N.R. Palapa, R. Mohadi, and A. Lesbani. "Adsorption of Direct Yellow Dye from Aqueous Solution by Ni/Al and Zn/Al Layered Double Hydroxides". AIP Conference Proceeding Series, 2026, 020018. 2018.

[15] S. Mallakpour, and M. Hatami. "Biosafe Organic Diacid Intercalated LDH/PVC Nanocomposites Versus Pure LDH and Organic Diacid Intercalated LDH: Synthesis, Characterization and Removal Behaviour of $Cd^{2+}$ from Aqueous Test Solution". Applied Clay Science, 149, 28–40. 2017.

[16] M. Xu, M. Bi, B. Xu, Z. Sun, L. Xu. "Polyoxometalate-Intercalated ZnAlFe-Layered Double Hydroxides for Adsorbing Removal and Photocatalytic Degradation of Cationic Dye". Applied Clay Science, 157, 86–91. 2018.

[17] R. Pourfaraj, S.J. Fatemi, S.Y. Kazemi, and P. Biparva. "Synthesis of Hexagonal Mesoporous MgAl LDH Nanoplatelets Adsorbent for the Effective Adsorption of Brilliant Yellow". Journal of Colloid and Interface Science, 508, 65–74. 2017.

[18] A. Lesbani et al., "Preparation and utilization of Keggin-type polyoxometalate intercalated Ni-Fe layered double hydroxides for enhanced adsorptive removal of cationic dye," SN Appl. Sci., vol. 2, p. 470, 2020.

[19] I.M. Ahmed, and M.S. Gasser. "Adsorption Study of Anionic Reactive Dye from Aqueous Solution to Mg-Fe-$CO_3$ Layered Double Hydroxide (LDH)". Applied Surface Science, 259, 650-656. 2012.

[20] R. Lafi, K. Charradi, M.A. Djebbi, A.B.H. Amara, and A. Hafiane. "Adsorption Study of Congo Red Dye from Aqueous Solution to Mg-AL-Layered Double Hydroxide". Advanced Powder Technology, 27, 232-237. 2016.

[21] C. Srilakshmi, and T. Thirunavukkarasu. "Enhanced Adsorption of Congo Red on Microwave Synthesized Layered Zn-Al Double Hydroxides and Its Adsorption Behaviour Using Moisture of Dyes from Aqueous Solution". Inorganic Chemistry Communications, 100, 107-117. 2019.

[22] Y.L. Long, J-G. Yu, F.P. Jiao and W.J. Yang. "Preparation and Characterization of MWCNTs/LDH Nanohybrids for Removal of Congo Red from Aqueous Solution". Trans. Nonferrous Met. Soc. China. 26, 2701-2710. 2016.

[23] W. Zhang, Y. Liang, J. Wang. Y. Zhang, Z. Gao, Y. Yang, K. Yang. "Ultrasound-Assisted Adsorption of Congo Red from Aqueous Solution Using Mg-Al.CO3 layered Double Hydroxide". Applied Clay Science, 174, 100-109. 2019.

[24]. A. Lesbani, and R. Mohadi. "Brönsted Acid of Keggin Type Polyoxometalate Catalyzed Pinacol Rearrangement". Bulletin Chemical Reaction Engineering and Catalysis, 9(2), 136-141.2019.

[25]. N. Ayawei, J. Godwin, and D. Wankasi. "Synthesis and Sorption Studies of the Degradation of Congo Red by Ni-Fe Layered Double Hydroxide". International Journal of Chemical Sciences, 13(3), 1197-1217. 2015.

[26]. H.N. Umh, and Y. Kim. "Sensitivity of nanoparticles' Stability at the Point of Zero Charge (PZC)". Journal of Industrial and Engineering Chemistry, 20 (5), 3175-3178. 2014.

[27] T. Taher, R. Mohadi, D. Rohendi, A. Lesbani. "Congo Red Removal from Aqueous Solution by Acid-Activated Bentonite From Sorolangun: Kinetic, Equilibrium, and Thermodynamic Studies". Arab Journal of Basic and Applied Sciences, 26 (1), 125-136. 2016.

[28] N. R. Palapa, R. Mohadi, A. Rachmat, and A. Lesbani, "Adsorption Study of Malachite Green Removal from Aqueous Solution Using Cu / M 3 + ( M 3 + = Al , Cr ) Layered Double Hydroxide," Mediterr. J. Chem., vol. 10, no. 1, pp. 33–45, 2020.

[29] L.B. Escudero, E. Agostini, G.L. Dotto. "Application of Tobacco Hairy Roots For the Removal of Malachite Green From Aqueous Solutions: Experimental Design, Kinetic, Equilibrium, and Thermodynamic Studies". Chemical Engineering Communications, 205, 122-133. 2018.

[30] S. Agarwal, F. Nekouei, H. Kargarzadeh, S. Nekouei, I. Tyagi, V.K. Gupta. "Preparation of Nickel Hydroxide Nanoplates Modified Activated Carbon For Malachite Green Removal From Solutions: Kinetic, Thermodynamic, Isotherm and Antibacterial Studies". Process Safety and Environmental Protection, 102, 85-97. 2016.

[31] A. Khataee, T.S. Rad, S. Nikzat, A. Hassani, M.H. Aslan, M. Kobya, and E. Demirbas. "Fabrication of NiFe

Layered Double Hydroxide/Reduced Graphene Oxide (NiFe-LDH/rGO) nanocomposite with Enhanced Sonophotocatalytic Activity for the Degradation of Moxifloxacin". Chemical Engineering Journal, 375, 122102. 2016.

[32] D.B. Jiang, C. Jing, Y. Yuan, L. Feng, X. Liu, F. Dong, and B. Dong. "2D-2D Growth of NiFe LDH Nanoflakes on Montmorillonite for Cationic and Anionic Dye Adsorption Performance". Journal of Colloid and Interface Science, 540, 398-409. 2019.

[33] D. Huang, J. Ma, L. Yu, D. Wu, K. Wang, M. Yang, D. Papoulis and S. Komarneni. "AgCl and BiOCl Composited with NiFe-LDH for Enhanced Photo-Degradation of Rhodamine B". Separation and Purification Technology, 156, 789-794. 2015.

[34] L. Kong, and H. Adidharma. "A New Adsorption Model Based on Generalized Van der Walls Partition Function for the Description of All Types Adsorption Isotherms". Chemica Engineering Journal, 375, 122112. 2019.